Development of Turbulence by the Interaction of Gas Flow with Plasmas

Lutz Niemeyer and Klaus Ragaller

Brown Boveri Research Center, CH-5401 Baden, Switzerland

(Z. Naturforsch. **28 a**, 1281–1289 [1973]; received 17 February 1973)

A high current electric arc in the axis of a supersonic nozzle flow is studied experimentally and theoretically in order to clarify the physical nature of light emission fluctuations which are observed inside the nozzle. The gas flow is produced by discharging a high pressure reservoir of 20 at N_2 through a nozzle of 12 mm throat diameter. The arc is fed with a rectangular current pulse of 1.9 kA amplitude and 5 ms duration. The light emission fluctuations of the arc are observed by photographic and photoelectric methods. The results of the observations are compared to theoretical estimates and lead to the conclusion that the fluctuations are caused by hydrodynamic turbulence. This turbulence is shown to be generated by the combined occurrence of a strong axial pressure gradient and a strong radial density gradient in the boundary layer between the arc and the surrounding cold gas flow. The influence of specific plasma properties on the character of the turbulence is briefly discussed from a theoretical point of view.

1. Introduction

In plasmas interacting with gas flows, fluctuations of the plasma light emission have been observed under various circumstances (e. g. Refs. [1–12]). The most detailed investigations in this field have been carried out on axially blown arcs, which occur for example in arc heaters. Special attention has been given here to current free plasma jets leaving arc heaters (Refs. [6–9]).

Only a few publications have, however, been devoted to the origin of the observed fluctuations. Kolonina [10] and Topham [11] assume hydrodynamic turbulence to start at the walls of the flow channel and to develop towards the arc, thus producing disturbations of the arc channel. Alternatively, Wutzke [12] showed that electrode spot movement may cause arc instabilities. Furthermore, electromagnetic instabilities of the arc column have been found to be responsible for the observed fluctuations [13].

In this paper we will demonstrate both theoretically and experimentally the existence of an additional effect that has not been previously investigated. This effect is principally present at the interaction of gas flows with plasmas and may cause hydrodynamic turbulence in the boundary layer between plasma and gas flow, leading to fluctuations of the plasma light emission. The experimental investigation of this effect has been carried out in a plasma flow configuration which has been specially designed to exclude all the other above mentioned mechanisms.

Reprint requests to Dr. L. Niemeyer, Gruppe Plasmaphysik, Brown, Bovery & Cie., AG, *CH-5401 Baden/Schweiz.*

2. Theoretical Discussion of the Turbulence-producing Mechanism

The general cause for the production of turbulence in hydrodynamic flow is vortex layers, i. e. flow regions with enhanced concentration of vorticity $\boldsymbol{\omega} = \nabla \times \boldsymbol{v}$ [14]. Under normal fluid mechanical conditions these vortex layers are generated by solid walls limiting the flow field. Their stability depends on the amount of vorticity production and on the Reynolds number which gives the ratio between convection and diffusion of vorticity [14]. A rather general stability criterion is the so called 'inflection point criterion', stating that a vortex layer is unstable whenever it leads to a velocity distribution with an inflection point.

This general argumentation will now be applied to the situation in which a gas flow interacts with a plasma. It will be shown that this interaction may produce vortex layers without solid walls being involved. This fact can be deduced from a slightly generalized form of the vorticity transport equation which in turn may be derived from the general Navier Stokes Equation:

$$\varrho \frac{\partial \boldsymbol{v}}{\partial t} + \varrho \nabla \left(\frac{v^2}{2} \right) - \varrho \, \boldsymbol{v} \times [\nabla \times \boldsymbol{v}] = - \nabla p + \boldsymbol{j} \times \boldsymbol{B} - \eta \nabla \times [\nabla \times \boldsymbol{v}]. \quad (1)$$

The viscous term in Eq (1) may be partially simplified assuming $\nabla \boldsymbol{v} = 0$ and $\eta(T) = \text{const}$, since the following discussion will be limited to large Reynolds numbers, i. e. small viscosity effects.

Applying the curl-operation to both sides of Eq. (1) one obtains

$$\frac{\partial \boldsymbol{\omega}}{\partial t} - \nabla \times [\boldsymbol{v} \times \boldsymbol{\omega}] - \frac{\eta}{\varrho} \Delta \boldsymbol{\omega} = -\nabla \times \left(\frac{\nabla p}{\varrho} \right) + \nabla \times \left[\frac{\boldsymbol{j} \times \boldsymbol{B}}{\varrho} \right] . \quad (2)$$

In order to demonstrate the essential effects we simplify Eq. (2) by specializing to situations in which $\boldsymbol{j} \times \boldsymbol{B}$ can be represented by $\nabla (\boldsymbol{B}^2/2\,\mu)$. The right hand side in Eq. (2) can then be written:

$$\nabla (\nabla p^*/\varrho) \quad \text{with} \quad p^* = p + B^2/2\,\mu$$

from which

$$(\partial \boldsymbol{\omega}/\partial t) - \nabla \times [\boldsymbol{v} \times \boldsymbol{\omega}] - (\eta/\varrho) \Delta \boldsymbol{\omega} = (1/\varrho^2) [\nabla \varrho \times \nabla p^*] = \boldsymbol{w} . \quad (3)$$

The left hand side of this equation corresponds to the well known transport equation of vorticity, the first term representing the temporal change at a fixed point in space, the second the change by convection, and the third viscous diffusion. On the right hand side, however, a new term $\boldsymbol{w}$ appears which is different from zero and represents a production of vorticity. This production occurs wherever a density gradient $\nabla \varrho$ subtends a non-zero angle with a pressure gradient ∇p^*.

A very high density gradient $\nabla \varrho$ is always present when a plasma interacts with a cold gas flow. The pressure gradient ∇p^* necessary for vorticity production may be generated in different ways, namely

(a) by being externally imposed,
(b) by the flow streaming around the plasma,
(c) by a magnetic pressure gradient.

Figure 1 gives two examples for illustration. Figure 1a shows an arc being stationarily stabilized against a cross flow by a transverse magnetic field. According to the last term in Eq. (3) vorticity is here produced parallel to the arc axis. Figure 1b shows an arc in the axial pressure gradient of a nozzle flow. Vorticity is seen to be generated at the boundary of the arc with vorticity lines azimuthally surrounding the arc.

The fact that vorticity may be produced in a free flow is of basic importance for the stability of the resulting vortex layers. As a consequence, from a fluid dynamic point of view, these vortex layers are closely related to free jets or wakes, the hydrodynamic stability of which has been subject to extensive study (Refs. [14–18]). It should be noted here that free vortex layers always lead to a velocity profile of the inflection point type and consequently

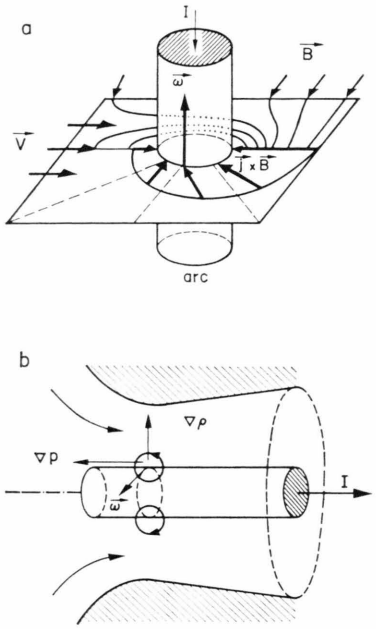

Fig. 1. Vorticity production by the interaction of an arc plasma column with a gas flow. a) Cross flow arc column stabilized by a transverse magnetic field. b) Axially blown arc column in an axial pressure gradient produced by a nozzle.

may become unstable at rather low Reynolds numbers Re. Thus, the situation in Fig. 1a corresponding to a wake behind a cylinder becomes unstable at $\mathrm{Re} > 50$ as related to the diameter of the cylinder [16]. A free jet corresponding to Fig. 1b becomes unstable at $\mathrm{Re} > 10$ as related to the thickness of the boundary layer [17]. This latter case forms the subject of this paper and will now be discussed in some detail.

As a starting point, the relevant Reynolds numbers in our experiment may be roughly estimated to be of the order $\mathrm{Re} \sim 5 \cdot 10^4$ thus greatly exceeding the critical value of $\mathrm{Re} \sim 10$. Consequently, the arc boundary layer is strongly unstable and should lead to turbulent vorticity production according to Equation (3).

In view of a more intuitive and qualitative understanding, this situation may be discussed in terms of integral quantities instead of the differential vorticity concept. From an integral point of view, the arc plasma has a flow velocity much higher than the surrounding cold gas flow. It is this velocity difference which gives rise to the unstable shear layer at the arc boundary. As this situation bears close resemblance to a submerged free jet the turbulence development should proceed in a way which is quali-

tatively similar to free jet turbulence. The characteristics of free jet turbulence are well known from the literature (e. g. Refs. [14–18]) and may be resumed as follows:

Turbulence sets on with certain modes which are found to be the most unstable ones in linear perturbation analysis. These modes generally exhibit a rather regular pattern. They usually consist of periodic sequences of azimuthal vortex rings which surround the jet in a more or less symmetric way. The resulting fluctuations are therefore rather periodic, i. e. they exhibit a frequency spectrum of rather narrow band type. As the initially generated perturbations are convected downstream the flow, they decay into finer modes at the same time loosing their regular pattern. This leads to a progressive broadening of the fluctuation spectrum towards higher frequencies. Finally, at a sufficient distance downstream from the point of onset, the turbulence pattern becomes totally irregular and a state of fully developed turbulence is reached.

3. Arc Experiment

Figure 2 shows a simplified diagram of the arc device used for our experiment, the details of which are described in Reference [19]. An electric arc is

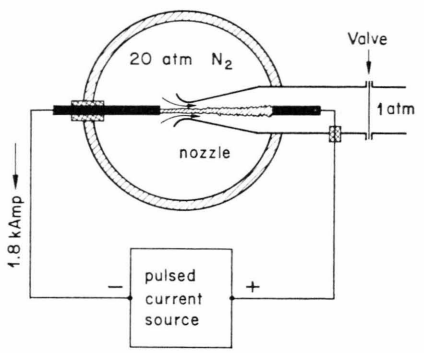

Fig. 2. Schematic diagram of axially blown arc experiment. Nozzle throat diameter: 12 mm, length: 100 mm, aperture angle: 8°.

ignited between two rod shaped electrodes and fed with a square current pulse of 1.9 kA amplitude and 5 ms duration. A supersonic axial flow of nitrogen is produced coaxially to the arc by a Laval nozzle with a throat diameter of 12 mm and a length of 100 mm. The gas pressure at the inlet of the nozzle is 20 atm expanding down to atmospheric pressure at the end and giving rise to a flow rate of 380 g/s. Because of the short duration of the experiment, the flow can be maintained from a high pressure tank with quiescent gas and practically constant pressure during the current pulse duration. Both the arc and the cold gas flow are found to attain stationary conditions after the first 3 ms of the current pulse so that a quasistationary situation prevails during a time interval of 2 ms.

It has been shown that this experiment does not exhibit any of the instabilities mentioned in Section 1. Thus, it can be assured that the gas streaming into the nozzle inlet is totally free of turbulence as the flow is fed from a volume of quiescent gas. This has been checked experimentally by schlieren observations of the region in front of the nozzle inlet. Secondly, special care has been taken to inhibit any magnetic instabilities of the arc column by properly dimensioning the upstream flow and electrode geometry. The complete stability of the arc column in this region may be seen from the streak record in Figure 3 a. Moreover, an interaction between the arc and the turbulent boundary layer on the nozzle wall had to be inhibited. This was achieved by properly adjusting the arc radius via the current such as to keep a sufficient distance between the arc boundary and the boundary layer on the wall. By computing the boundary layer thickness according to [20a] it is found not to exceed a fraction of a mm even 20 mm downstream of the nozzle throat. This fact has been confirmed experimentally by schlieren observations [20b].

A compilation of the most important measured quantities of the arc, such as temperature, velocity, pressure, and electric field strength distributions may be found in Refs. [21] and [22].

4. Measurement of Light Emission Fluctuations

The light emission fluctuations of the arc plasma have been observed by two experimental methods, namely photographics treak records and photoelectric intensity measurements. The streak records yield a general qualitative survey about the structure and spatial distribution of the fluctuations, whereas the photoelectric measurements supply time signals that are quantitatively evaluated with respect to their statistical characteristics.

4.1. Streak records

Fast streak records of the arc cross section have been taken side-on at different axial positions along the nozzle axis. For this purpose the nozzle has been provided with small azimuthal observation slits and quartz windows. A set of typical streak records is

given in Figure 3. From Figs. 3 a and b it is seen that the arc is totally free of perturbations from the region outside of the nozzle down to the nozzle throat. The fluctuations observed further downstream from this point (Fig. 3 c – f) can therefore not be introduced from outside, neither by the cold gas flow nor by some arc instability. Fluctuations of the arc emission first appear in Fig. 3 c, i. e. some 15 mm downstream from the nozzle throat. Consequently

(I) the axial point of onset of the fluctuations is localized somewhere within the first 15 mm downstream of the nozzle throat.

Figure 3 c shows that the fluctuations are, at this point, predominantly confined to the arc boundary whereas they progressively penetrate into the interior of the arc further downstream (Figures 3 d – f). Consequently,

(II) the origin of the fluctuations is located in the boundary region between the arc and the surrounding cold gas flow.

The light emission fluctuations possess a rather irregular pattern which is strongest in the downstream portion of the nozzle. Large scale motions of the integral arc as they are known from magnetic arc instabilities do not occur. Consequently, the observed fluctuations are not produced by this kind of instability.

4.2. Photoelectric Measurements

The photoelectric measurement setup is shown in Figure 4. Two beams of observation 1 and 2 are focused perpendicular to the arc axis to measure light emission fluctuations at two axial positions separated by a distance Δz. The light to be measured is spectrally filtered by the filters F* and sensed by photomultipliers PM. The fluctuating components of the multiplier signals are amplified and fed into fast digital transient recorders of type Biomation 610 B, from where they are punched out on paper tape for subsequent numerical evaluation by a computer. The diameter of the beams of observation is less than 0.4 mm, i. e. small compared to the arc diameter 2R which is typically 5 – 10 mm. The axial distance Δz between the two beams has been varied between 3 and 9 mm. The overall frequency range of the measuring equipment extends from

* 1000 Å bandpass filters centered at 4500 Å. In this spectral region, the emission coefficient of the arc plasma is predominantly determined by continuum radiation.

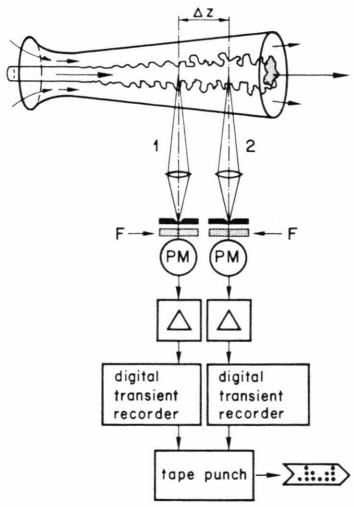

Fig. 4. Photoelectric fluctuation measurement setup. 1,2: beams of observation, F: spectral filters 4000 – 5000 Å, PM: photomultipliers.

50 kHz to 3 MHz. The measurements have been made at different positions z along the nozzle axis.

It should be stressed that these measurements only provide information about the total intensity fluctuations along the beams of observation, i. e. along the arc diameter. All conclusions drawn from these measurements must therefore be regarded as averaged across the total luminous plasma column diameter.

The statistical properties of the fluctuation signals have been evaluated with respect to those quantities which have proven valuable for the description of turbulence phenomena, namely correlation functions and spectral power density distributions.

The *space time correlation function* of two fluctuation signals $i_1(t)$ and $i_2(t)$ measured at two different axial positions z and $z+\Delta z$ is defined by

$$\varphi(\Delta z, \tau) = \frac{\langle i_1(z,t)\, i_2(z+\Delta z, t+\tau)\rangle}{(\langle i_1(t)^2\rangle \langle i_2(t)^2\rangle)^{1/2}}$$

where $\langle\,\rangle$ indicates time averaging.

Figure 5 gives some examples of the kind of correlation functions obtained from measurements taken in the strongly fluctuating arc portion near the downstream end of the nozzle. The axial separations of the measuring beams are $\Delta z = 0$ (autocorrelation function), $\Delta z = 3$ mm and $\Delta z = 6$ mm. These correlation functions show two distinctive properties:

a) For a fixed value of Δz, the time correlation functions exhibit a pronounced maximum at a time

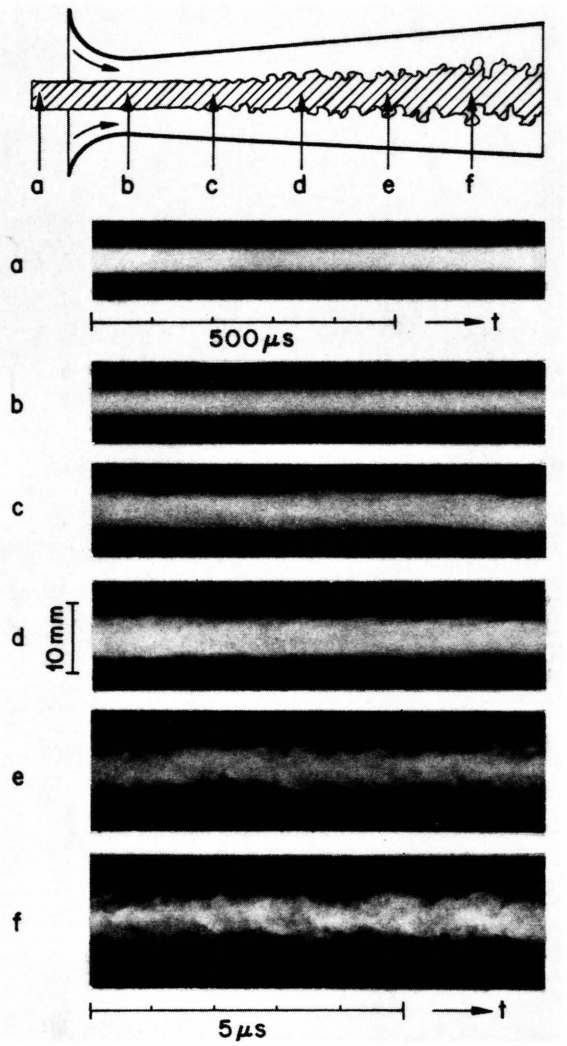

Fig. 3. Fast streak records of the nozzle cross sections at different axial positions along the nozzle axis.

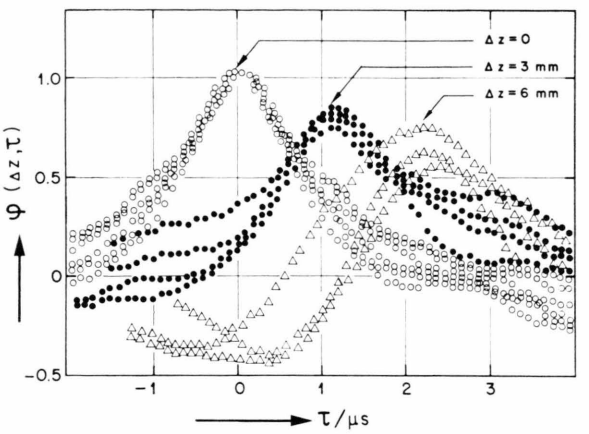

Fig. 5. Correlation functions $\varphi(\Delta z, \tau)$ measured near the downstream end of the nozzle with different axial distances Δz between the beams of observation.

delay $\tau = \tau_0$ which is proportional to the beam separation Δz. This time delay indicates the transit time of the fluctuation elements during their axial flow motion across the distance Δz. The average axial velocity v_z of the fluctuation elements may therefore be calculated as $v_z = \Delta z/\tau_0$. The evaluation of this relation yields the average axial flow velocity of the arc region at different axial positions z as represented in Figure 6.

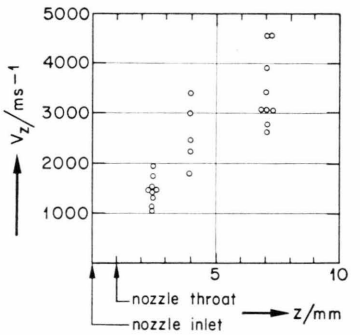

Fig. 6. Axial distribution of average axial flow velocity v_z in the arc as determined from correlation measurements.

b) The Δz-dependence of the maximal correlation amplitude $\varphi(\Delta z, \tau_0)$, i. e. the spatial correlation function $\varphi(\Delta z)$ is found to decay monotonously with increasing axial separation Δz between the measuring beams. This behaviour is illustrated by Figure 7, the data being obtained in the arc portion near the downstream end of the nozzle. The spatial correlation function is seen to decay monotonously to zero over a length of order $\lambda_z \sim 1$ mm. This is the axial correlation length and indicates the distance overw hich the fluctuation elements preserve their identity before they decay. Thus:

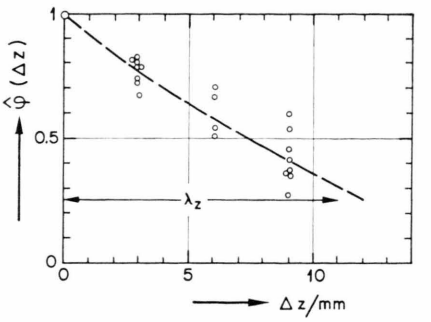

Fig. 7. Spatial correlation function $\varphi(\Delta z)$ in the direction z of the nozzle axis as determined from fluctuation measurements near the downstream end of the nozzle. λ_z: order of magnitude of the axial correlation length.

(III) the axial correlation length of the fluctuation elements is of the order of $\lambda_z \sim 10$ mm.

The second important statistical quantity to be evaluated from the fluctuation signals is the spectral power density distribution $S(f)$ which is defined by the squared Fourier transform of the fluctuation time signal $i(t): S(f) = F\{i(t)\}^* F\{i(t)\}$ or alternatively, according to the Wiener formula by $S(f) = F\{\varphi(0, \tau)\}$ where $\varphi(0, \tau)$ is the autocorrelation function of the fluctuation signal, and $F\{\}$ indicates the Fourier transform operator.

$S(f)$ gives an indication of the intensities, with which different fluctuation frequencies are present in the signal. As an example the power spectra measured at three axial positions z along the nozzle are displayed in Figure 8. Comparing these spectra, the following conclusions may be drawn:

(IV) The spectrum in the region of onset of fluctuations (Fig. 8 a) has a comparatively narrow bandwidth and shows a relatively sharp decrease towards high frequencies. Towards the downstreams end of the nozzle the high frequency portion of the spectrum grows appreciately (Figs. 8 b and c). As an example at $f = 1$ MHz the relative power grows about one order of magnitude from the region of onset (Fig. 8 a) to the nozzle end (Figure 8 c).

5. Interpretation of the Measurements

In order to demonstrate that the observed fluctuation phenomena are caused by the type of turbulence postulated in Section 2, we shall now show that the theoretically postulated characteristics of

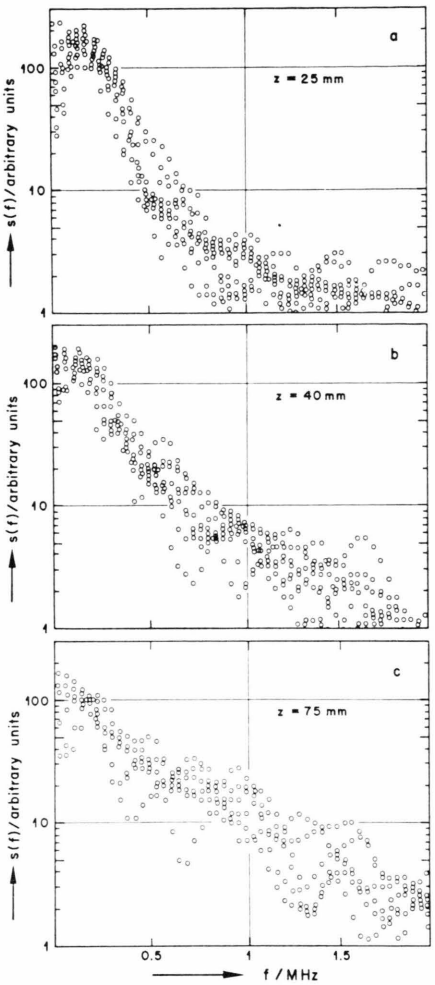

Fig. 8. Fluctuation power spectra $S(f)$ measured at different axial positions in the nozzle. a: 15 mm downstream of the nozzle throat. b: 30 mm downstream of the nozzle throat. c: 60 mm downstream of the nozzle throat.

this turbulence are in order of magnitude agreement with the observations. A more quantitative comparison will only be possible on the basis of more refined, locally resolved measurements which will be published in a subsequent paper.

5.1. Onset of Turbulence

According to the arguments given in Section 2 the present flow configuration leads to turbulent vorticity production in the boundary layer between the arc and the surrounding cold gas flow. In order to determine the point of onset of turbulence the axial distribution of the vorticity production term $\boldsymbol{w}(z) = \varrho^{-2}[\nabla\varrho \times \nabla p]$ in Eq. (3) has to be inspected. An approximate calculation of this quantity from measured temperature, pressure, and density distributions yields the result display in Fig. 9 together with the nozzle contour $R(z)$. The vorticity

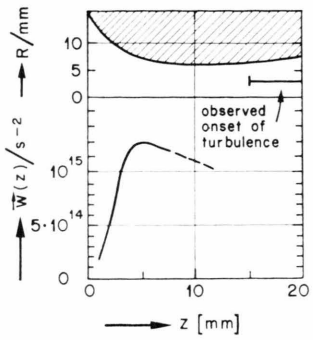

Fig. 9. Nozzle contour $R(z)$ and approximately calculated axial distribution of the vorticity production term $\boldsymbol{w}(z) = \varrho^{-2}[\nabla\varrho \times \nabla p]$.

production $\boldsymbol{w}$ is seen to rise steeply in the nozzle inlet region reaching a maximum in the vicinity of the nozzle throat. Consequently the onset of turbulence would be expected around this point. The exact determination of the point of onset is, however, one of the unsolved problems of turbulence theory. Until now it is only known that a certain delay may exist between the so-called point of indifference, where the flow situation just begins to become unstable and the real onset of turbulence. The point of onset may therefore be extended some distance downstream of the vorticity production region, i. e. in the downstream vicinity of the nozzle throat. This conclusion agrees with the observation (I) in section 4.2.

Another consequence of the vorticity production concept is that the turbulence should develop out of the unstable boundary layer between the arc and the surrounding cold gas flow. This consequence is confirmed by the observation (II) of Section 4.1.

As has been pointed out in Section 2, the present flow configuration is best compared to turbulent free jets. The free jet turbulence results may, however, be applied to the present situation only in a qualitative manner as the relevant parameters such as Mach number, pressure, and density gradients are not comparable. Free jet turbulence is known to start with disturbances prefering a rather narrow frequency band. In the region of onset, the fluctuation spectrum should therefore have a comparatively bandwidth. Downstream narrow, however, it should

progressively grow out towards higher frequencies due to the decay of the initial perturbations into finer turbulence eddies. This behavior is in fact confirmed by the measured fluctuation spectra [(IV) in Section 4.2. and Figure 8].

5.2. Fully Developed Turbulence Near the Downstream End of the Nozzle

As has been pointed out in Section 2, free jet turbulence tends to develop towards a state of fully developed turbulence in a region sufficiently far downstream from the point of onset. The strongly irregular character of the fluctuations near the downstream end of the nozzle leads to the assumption that this state has been approximately reached at this point.

A broad experimental and theoretical literature exists on this special type of turbulence. In view of the order of magnitude character of our observations, we will, however, restrict our discussion to order of magnitude estimates which may be derived by dimensional analysis [23]. One of the results obtained in this way is the relation

$$\lambda_z \sim L \sim D$$

where λ_z is the spatial correlation length, L the macroscale, i. e. the scale of the most strongly excited turbulence eddies and D the scale of the flow field. Comparing the value of $\lambda_z \sim 10$ mm determined from the correlation measurements [(III) in Section 4.2)], to the nozzle radius $R \sim 10$ mm, which characterizes the scale of the flow field one obtains an order of magnitude agreement indicating that in fact a state near to fully developed turbulence has been reached.

It would be interesting to extend the comparison to the microscale l of the turbulence which gives the scale of the smallest eddies as determined by viscous dissipation. Dimensional analysis yields:

$$l \sim (\nu L^{1/3}/\Delta v)^{3/4}$$

Here $\nu = \eta/\varrho$ is the kinematic viscosity and Δv the variation of the mean velocity across the flow field. Taking as rough estimates $\nu \sim 1\ \mathrm{cm^2/s}$ and $v \sim 2000$ m/s one obtains fluctuation frequencies $f_{\max} \sim v/l$ in the 100 MHz range. These are beyond the scope of our measurement capabilities, so that no comparison can be made.

Resuming the above discussion it may be concluded that the observed light emission fluctuations are caused by hydrodynamic turbulence which starts from the hydrodynamically unstable arc boundary layer in the vicinity of the nozzle throat and grows towards a fully developed state near the downstream end of the nozzle.

6. Influence of Specific Plasma Properties on the Turbulence

The previous discussion has been based on order of magnitude comparisons and has enabled us to understand the basic nature of the observed light emission fluctuations in a qualitative way. The actual conditions in the arc nozzle flow differ, however, appreciably from the conditions in ordinary hydrodynamic turbulence because of the particular properties of the plasma involved. It should therefore not be surprising to find strong deviations when conducting a more quantitative comparison. There is, in fact, some evidence for such deviations, and we will discuss now, from a theoretical point of view, some effects which may be responsible for a specifically different behavior of the turbulence in the presence of a plasma.

The starting point of the discussion is the energy balance equation for the turbulent kinetic energy [24], which may be derived from the basic fluid dynamic equations by dividing all quantities involved into average values and fluctuations in the following manner:

$$p = \langle p \rangle + p', \quad v = \langle v \rangle + v',$$
$$\tilde{v} = \langle \varrho\, v \rangle / \langle \varrho \rangle, \quad \tau = \langle \tau \rangle + \tau'$$

where the quantities in brackets are time averages and the primes indicate fluctuations. τ is the viscous stress tensor. Using the common index notation, one obtains:

$$\begin{aligned} \frac{\partial}{\partial x_j}\left\langle \frac{1}{2}\varrho\, v_i' v_j' \right\rangle \tilde{v}_j = &-\left\langle v_j' \frac{\partial p}{\partial x_j} \right\rangle \\ &- \langle \varrho\, v_i' v_j' \rangle \frac{\partial \tilde{v}_j}{\partial x_j} + \frac{\partial}{\partial x_j}\langle v_i' \tau_{ij} \rangle \\ &- \frac{\partial}{\partial x_j}\left\langle v_i' \frac{1}{2}\varrho\, v_i' v_j' \right\rangle - \left\langle \tau_{ij} \frac{\partial v_i'}{\partial x_j'} \right\rangle . \end{aligned} \tag{4}$$

In this expression, magnetic forces have been neglected. This is justified if the Cowling number $C = B^2/\mu\, \varrho\, v^2$ and the magnetic Reynolds number $R_m = \sigma\, \mu\, v\, L$ are small compared to unity, a condition that is well fulfilled in our case. Turbulence under strong influence of magnetic fields has been investigated in Reference [25].

The left hand side of Eq. (4) describes the convective transport of kinetic turbulent energy with the mean flow and the right hand side gives the production and dissipation terms. This equation has been thoroughly discussed in the literature and has been verified experimentally.

We are now going to study how specific plasma properties may influence the terms in this equation and produce characteristic deviations from ordinary hydrodynamic turbulence.

One obvious effect of this kind is the strong local variation of the viscous stress τ_{ij}, which is caused by the temperature dependence of the viscosity. This results in an additional contribution to the third term on the right hand side of Eq. (4), which would be absent in purely hydrodynamic flow, namely

$$\partial/\partial x_j \langle v_i' \tau_{ij} \rangle .$$

As has been stated above, viscosity has its main influence on the high frequency portion of the turbulence spectrum. Thus, deviations are to be expected in this spectral region.

The remaining terms of Eq. (4) are all present in ordinary hydrodynamic turbulence, too. Deviations, caused by the plasma should therefore be sought in these terms. A special effect of importance in our case, shall be briefly discussed. If an electric current is imposed on the plasma, then the conducting path between the electrodes must not be interrupted. Consequently, all turbulent flow modes which would lead to such an interruption are disallowed. Therefore, contrary to the commonly used colour filament experiments in fluids, a 'plasma filament' must be kept intact. This effect enters into Eq. (4) via the first term on the right hand side.

We shall illustrate the corresponding physical mechanism with the example sketched in Fig. 10, in which the current carrying arc plasma column is shown together with one of the possible vortex rings

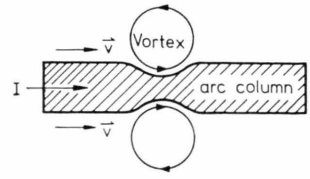

Fig. 10. Interaction of an azimuthal cold gas vortex ring with the arc column.

in the cold gas flow. This vortex ring is tending to narrow the arc column thus causing the electric field strength to grow. This, in turn, causes enhanced Joule heating, as the imposed current is kept unchanged. This enhanced Joule heating then leads to a relative movement between the isothermal surfaces of the arc and the cold gas flow of the vortex which is therefore hindered to push the plasma forward like a fluid of different colour. Whenever this relative movement takes place, i. e. when cold gas is heated, correlated pressure and velocity fluctuations should occur and give a contribution to the first term in Eq. (4), which then describes the hindering of this motion. This effect is currently being investigated in our experiment.

Acknowledgements

The theoretical arguments in this work have benefitted from clarifying discussions with L. S. Dzung. Important experimental advice has been given by O. E. Lanz.

[1] W. Fischer-Schlemm and P. A. Schoeck, Oscillations of Electric Arcs with Superimposed Gas Flow, Proceedings of the seventh International Conference on Phenomena in Ionized Gases, Vol. I, Beograd 1966, p. 720.
[2] M. P. Freeman and U. L. Sik, J. Appl. Phys. **33**, (No. 9) 2845 [1962].
[3] D. M. Benenson, C. H. Naeher, and J. B. Gideon, AIAA J. **5**, (No. 8) 1517 [1967].
[4] H. Fischer and K. Schoenbach, Turbulent Eddies in High-Density-Spark Channels in Helium, AFCRL 670544, Sept. 1967, Air Force Cambridge Research Labs.
[5] G. Frind and B. L. Damsky, Electric Arcs in Turbulent Flows, IV, ARL 70-0001, Jan. 1970, Aerospace Research Labs.
[6] J. Grey and P. F. Jacobs, AIAA J. **2**, (No. 3) 433 [1964].
[7] T. J. O'Connor, E. H. Comfort, and L. A. Cass, AIAA J. **4**, (No. 11) 2026 [1966].
[8] A. Demetriades and E. L. Doughman, AIAA J. **7**, (No. 4) 713 [1969].
[9] V. A. Gulubev, High Temperature Turbulent Jets, in Turbulent Jets of Air, Plasma and Real Gas, G. N. Abramovich ed., Consultants Bureau, New York 1969, pp. 1–36.
[10] L. I. Kolonina and B. A. Uriukov, Electric Arc Intensity in the Region of Interaction with a Turbulent Boudary Layer in a Vortex-Stabilized Plasmatron, Akademiia Nauk SSSR, Sibirskoe Otdelenie, Izvestiia, Seriia Tekhnicheskich Nauk, Oct. 1968, pp. 28–32.
[11] D. Topham, The Aerodynamics of Electric Arcs in Axial Flow, Ph.D. Thesis, Loughborough University of Technology, June 1970.
[12] S. A. Wutzke, E. Pfender, and E. R. G. Eckert, AIAA J. **5**, (No. 4) 707 [1967].
[13] J. K. Harves, P. G. Simpkins, and B. D. Adcock, Instability of Arc Columns, AIAA J. **1**, (No. 3) 714 [1963].
[14] L. Rosenhead, Ed., Laminar Boundary Layers, Fluid Motion Memoirs, Clarendon Press, Oxford 1963, Chapter II.
[15] S. Chandrasekhar, Hydrodynamic and Hydromagnetic Stability, Clarendon Press, Oxford 1968, Chapter XII.

[16] H. Schlichting, Grenzschichttheorie, 5th ed., G. Braun, Karlsruhe 1965, Chapter XX.
[17] F. K. Moore, Ed., Theory of Laminar Flows, in High Speed Aerodynamics and Jet Propulsion, Vol. IV, Princeton University Press, 1964, Chapter G.
[18] A. Michalke, The Instability of Free Shear Layers, a Survey of the State of Art, DRL Mitt. 70-04, March 1970, Deutsche Forschg.- und Versuchsanst. f. Luft- und Raumfahrt.
[19] W. Bötticher, U, Kogelschatz, and E. Schade, Z. Naturforsch. **27 a**, 1433 [1972].
[20a] H. Schlichting and E. Truckenbrodt, Aerodynamik des Flugzeugs, 2nd ed., Springer-Verlag, Berlin 1962, Chapter IV.
[20b] U. Kogelschatz, private communication.
[21] U. Kogelschatz and E. Schade, Experimental Investigation of a High Pressure Arc in a Strong Axial Gas Flow, 10th International Conference on Phenomena in Ionized Gases, Oxford 1971, p. 198.
[22] W. Hermann and K. Ragaller, Theory of the High Pressure Arc in a Strong Axial Gas Flow, 10th International Conference on Phenomena in Ionized Gases, Oxford 1971, p. 199.
[23] L. D. Landau and E. M. Lifshitz, Course of Theoretical Physics, Vol. 6 Fluid Mechanics, 2nd ed., Pergamon Press, Oxford 1963, Chapter III.
[24] J. Laufer, Lecture on Turbulence, held at the ETH Zurich, Switzerland, May 1971.
[25] S. I. Pai, Magnetogasdynamics and Plasma Dynamics, Springer, Vienna 1962, Chapter VIII.

On the Determination of Electron Temperature in Diffusion-Dominated Non-L.T.E. Plasmas

H. W. Drawin and F. Emard

Association EURATOM-CEA sur la Fusion
Département de Physique du Plasma et de la Fusion Contrôlée
Centre d'Etudes Nucléaires
92260 Fontenay-aux-Roses (France)

(Z. Naturforsch. **28 a**, 1289–1293 [1973]; received 12 February 1973)

Population densities of atomic hydrogen levels have been calculated for homogeneous stationary and diffusion-dominated stationary plasmas. The results show strong overpopulation of the lower lying excited states when the actual number density of ground state atoms is larger than the density obtained for the homogeneous stationary state. At low electron and high ground state densities the so-called Boltzmann slope is not further a characteristic quantity for the determination of electron temperatures, since the slope constant changes with quantum number. — The partial L.T.E. condition for diffusion-dominated plasmas is reexamined.

Introduction

Spectroscopic measurements of line emission coefficients made by different authors on wall-stabilized arcs operated at relatively high pressures [1–5] and on high-temperature magnetically confined vacuum arcs [6–8] have shown over- and underpopulations for a limited or a large number of quantum states $|i\rangle$ when compared with the Saha density n_i^{Saha} given by the relation

$$n_i^{\mathrm{Saha}} = n_+ \, n_e \frac{g_i}{2\, g_+} \frac{h^3}{(2\pi m_e k T_e)^{3/2}} \exp \frac{E_i - \nabla E}{k T_e} \tag{1}$$

and when compared with the Boltzmann population density $n_i^{\mathrm{Boltzm.}}$ based on the complete L.T.E. assumption. Population densities n_i satisfying Eq. (1) are said to be in partial L.T.E. The electron temperature T_e of a non-L.T.E. plasma can be determined from a Boltzmann plot when only levels i are considered which are in partial L.T.E. with respect to n_e and T_e (which implicitely means that only electronic collisions are responsible in populating and depopulating these levels). We show in the following that strong diffusion may destroy any possibility of determining electron temperatures from a "Boltzmann plot", since the diffusion effect pushes the usual partial L.T.E. condition to so high quantum levels that it becomes impossible to determine the slope of the Boltzmann plot with sufficient precision.

Reprint requests to Dr. H.-W. Drawin, Association Euratom-CEA sur la Fusion, Département de Physique du Plasma, Centre d'Etudes Nucléaires, Boite Postale nº 6, *F-92260 Fontenay-aux-Roses*, France.

General Form of Rate Equations and their Solutions

We consider the level system of atomic hydrogen. The number density n_i of the i-th level (in the following i denotes the principal quantum number) is given by the relation

$$\partial n_i/\partial t + \nabla \cdot (n_i \bar{v}_i) = (\partial n_i/\partial t)_{\mathrm{coll,\,rad}}\,, \qquad i = 1, 2, 3, \ldots, p \tag{2}$$